Simplified Models for Plume Dynamics: Simulation Studies for Geological CO_2 Storage Certification Framework

Authors: Navanit Kumar, Steven.L.Bryant, J.P. Nicot; University of Texas at Austin and Curtis M. Oldenburg, Lawrence Berkley National Laboratory

Abstract:
A critical requirement for large-scale deployment of CO_2 sequestration in brine formations is a framework for certifying and decommissioning sites. As part of the development of such a framework, we are conducting a series of simulations to evaluate ranges of CO_2 plume behavior as a function of reservoir and operating parameters. The objective is to describe key features of the plume behavior with highly simplified models that can be integrated into the framework.
.

Three-dimensional simulations are carried out using CMG-GEM simulator. Reservoir parameters studied are porosity, permeability, anisotropy, thickness, dip, pressure and potential leakage through faults. The operating parameters studied are injection rate, vertical vs horizontal well and perforation interval.

Simulation results are classified into three response variables that correspond to several aspects of leakage risk: total amount of free gas in the reservoir, maximum lateral distance traveled, and time the plume takes to reach the top seal. The effect of parameters on each of the response variables strongly depends on other reservoir properties. For example, in a thick homogeneous reservoir, dip is beneficial because it increases the mobility of CO_2 and thus enhances trapping of CO_2 by dissolution in the aqueous phase and by residual saturation. On the other hand in thin and faulted reservoirs, dip enables the plume to reach the top seal, then travel rapidly to a distant fault or abandoned well which can act as a leakage conduit. A horizontal well may offer sufficient reduction in leakage risk compared to a vertical well to overcome the additional cost of drilling and completing. The perforation interval in both vertical and horizontal wells can be optimized for a given rate of injection. A semi- analytical model is discussed for optimized perforated intervals.

Simplified analytical models are discussed for plume velocity in dipping and non-dipping aquifers which can predict the time to hit top seal for a given set of reservoir and operating dimensionless parameters.

Introduction

A certification framework is a tool to commission geological sites for CO_2 sequestration. The objective is to develop a simple and transparent framework acceptable to key stakeholders for evaluating the risk that CO2 leakage would impose on resources and environment. One step toward this goal is developing scenarios for the most likely reservoir types to be used for CO2 storage, modeling and simulation of the scenarios and calculating the associated

probabilities of CO_2 leakage. Potential leakage paths include the top seal, abandoned wells and faults. Leakage risk is classified into three response variables- time the plume takes to reach top seal, maximum lateral extent and total mobile gas. Simulation studies are performed to see the effect of various reservoir parameters and operating parameters on the above three response variables. This paper also describes simplified models of migration dipping reservoirs and reservoirs with distributed shale barriers.

Simulation Outline

The mechanisms for trapping CO2 in aquifers include dissolution in brine, residual saturation and mineralization. The simulations discussed here account for the first two mechanisms but do not include mineralization. Three dimensional compositional simulations are carried out using CMG-GEM as described in Kumar et al (2004). For phase behavior of the CO_2-brine system, Peng-Robinson EOS is used and parameters are tuned to match experimental data. Constant pressure boundary condition is applied by placing production wells all around boundary operating at constant BHP of initial reservoir pressure. Hysteresis in relative permeability due to co-current and then counter-current flow is modeled using Land's hysteresis model.

Effect of individual parameters

Porosity: The lower the porosity, the lower is the brine available to dissolve CO_2. Also the interstitial velocity decreases with increase in porosity. But lower porosity is generally associated with higher residual gas saturation. Holtz (2002) fit data on various measurements to the correlation

$$S_{grm} = -0.9696\phi + 0.5473$$

The combined effect of above mechanisms depends upon rate of injection and solubility of CO2 in brine at reservoir conditions.

Permeability: Higher permeability lowers the injection pressure required. If injection occurs at constant pressure, the plume moves faster due to lower resistance to flow. Lower injection pressure also decreases the density of CO2 and thus increases the buoyant flow.

Permeability Anisotropy: Permeability anisotropy is the most sensitive parameter for all of the three response variables. The higher the value of Kv/Kh, the less would be the time for the plume to reach the top seal. Once it reaches the top, the CO_2 plume will spread rapidly underneath the seal, increasing the probability of encountering a leakage path. As the CO_2 rises it establishes a high saturation (high gas relative permeability) path, which becomes a preferential channel for continued CO_2 migration. This reduces the volume of rock and brine

contacted with CO_2 and thus reduces trapping. Therefore higher Kv/Kh is detrimental in terms of all of the response variables.

Dip: Dip increases the lateral extent of CO_2 plume in updip direction. On the other hand it increases the trapping of CO_2. One reason is that in dipping reservoirs the plume is traveling longer distance before reaching the top seal, thereby trapping a greater amount of CO_2 as residual saturation. Another reason is that CO_2 comes into contact with more unsaturated brine which will enhance dissolution. But once the plume hits the top seal it moves fast in updip direction, increasing further the lateral extent and decreasing trapping.

An analytical study is performed to find the effect of dip on flux magnitude and resultant direction. The schematic of plume movement in dipping reservoir is shown in Figure 1. For two phase flow

$$S_g + S_w = 1 \qquad \text{....1}$$

From Darcy law

$$u_g = -\frac{k_x k_{rg}}{\mu_g}\left(\frac{\partial P_g}{\partial x} + \rho_g g \sin\alpha\right) \qquad \text{.....2}$$

$$u_w = -\frac{k_x k_{rw}}{\mu_w}\left(\frac{\partial P_w}{\partial x} + \rho_w g \sin\alpha\right) \qquad \text{.....3}$$

Capillary pressure is defined as

$$P_c = P_g - P_w$$

Total flux is given by

$$u_t = u_g + u_w$$

$$u_g = u_t + \frac{k_x k_{rw}}{\mu_w}\left(\frac{\partial P_g}{\partial x} - \frac{\partial P_c}{\partial x} + \rho_w g \sin\alpha\right)$$

Substituting $\frac{\partial P_g}{\partial x}$ from equation 2 and rearranging

$$u_g = \left(\frac{\lambda_{rg}}{\lambda_{rg} + \lambda_{rw}}\right)\left(u_t + k_x \lambda_{rw}\left(\Delta\rho g \sin\alpha - \frac{\partial P_c}{\partial x}\right)\right)$$

where $\lambda_{rg} = \frac{k_{rg}}{\mu_g}$

For countercurrent flow

u_t =0

$$u_g = \left(\frac{\lambda_{rg}}{\lambda_{rg} + \lambda_{rw}}\right)\left(k_x \lambda_{rw}\left(\Delta\rho g \sin\alpha - \frac{\partial P_c}{\partial x}\right)\right)$$

Similarly for vertical flow

$$u_{gv} = \left(\frac{\lambda_{rg}}{\lambda_{rg} + \lambda_{rw}} \right) \left(k_v \lambda_{rw} \left(\Delta\rho g - \frac{\partial P_c}{\partial v} \right) \right)$$

assuming relative permeability in dip direction to be same as in vertical direction and that the frontal saturation in both directions is same. Thus

$$\left(\frac{u_{gx}}{u_{gv}} \right)_f = \frac{k_x \lambda_{rw} \left(\Delta\rho g \sin\alpha - \frac{\partial P_c}{\partial x} \right)}{k_v \lambda_{rw} \left(\Delta\rho g - \frac{\partial P_c}{\partial v} \right)}$$

$$u = \sqrt{u_x^2 + u_v^2 + 2u_x u_v \sin\alpha}$$

where u is the resultant vector at angle θ from dip direction given by

$$\cos\theta = \frac{u_x + u_v \sin\alpha}{u}$$

Figure 2 shows the above derived ratio of flux in dipping direction to flux in vertical direction as a function of permeability anisotropy and dip angle. These simple equations can be used to estimate the response variables.

Managing Shale Barrier with equivalent homogeneous system

Haldorsen and Lake (1984) have described shale management schemes in field scale modeling. Weber (198x) presented an empirical relationship between shale continuity and depositional environment. Marine depositions show highest continuity and the point bar the lowest. Estimating the continuity of shales from depositional environment and net-to-gross (ratio of total thickness of permeable strata within the aquifer to the overall aquifer thickness) from the well log, a simplified equivalent homogeneous medium can be obtained for certification framework. The concept of "equivalent" here means finding the permeability anisotropy in a homogeneous medium that yields the same time for the plume to reach the top as in the actual medium. Figure 3 shows the schematic of the tortuous paths taken by a buoyant plume in a reservoir with imbedded shale barriers. We can derive a simple formula for the travel time to the top of the formation as follows

Vertical flux from the injection well: $u_{v1} = -\frac{k_v}{\mu} \left(\frac{\partial P}{\partial v} + \rho_g g \right)$

Time plume takes to reach the barrier from top perforation

$$t_1 = \frac{h}{u_{v1}}$$

Similarly, the horizontal flux is given by $u_{h1} = -\frac{k_h}{\mu}\left(\frac{\partial P}{\partial x}\right)$

and the time to reach the edge of the shale barrier is $t_2 = \frac{L}{u_{h1}}$

Now if L is large, the path of plume after reaching tip of barrier is dominated by buoyancy flow.

$$u_{v3} = -\frac{k_v}{\mu}\left((\rho_g - \rho_w)g\right)$$

Thus the time to travel from tip of barrier to top seal is

$$t_3 = \frac{H-h}{u_{v3}}$$

For the equivalent homogeneous system, time to reach top seal is

$$t = \frac{H}{u'_v}$$

where $u'_v = -\frac{k'_v}{\mu}\left(\frac{\partial P}{\partial v} + \rho_g g\right)$

Equating the times to reach top seal

$$t = t_1 + t_2 + t_3$$

we find

$$\frac{H}{u'_v} = \frac{h}{u_{v1}} + \frac{L}{u_{h1}} + \frac{H-h}{u_{v3}}$$

Replacing flux terms from corresponding Darcy law formulation and assuming $\frac{\partial P}{\partial x} \approx \frac{\partial P}{\partial v}$ near well bore we get

$$\frac{k'_v}{k_h} = \frac{\frac{k_v}{k_h} N_g H}{hN_g + L\left(\frac{k_v}{k_h}\right)\left(1 + \frac{\rho_g g}{\frac{\partial P}{\partial x}}\right)N_g + (H-h)\left(1 + \frac{\rho_g g}{\frac{\partial P}{\partial x}}\right)}$$

We can then compute a dimensionless group convenient for characterizing this type of displacement (Ide et al., 2006):

$$N_g = \left(\frac{\Delta\rho g}{\frac{\partial P}{\partial x}}\right) = \frac{k\Delta\rho g}{\mu u}$$

where N_g is the gravity number, the ratio of gravity forces and viscous forces.

Figure 4 compares the time to hit the top for plume in imbedded shale aquifer and its equivalent homogeneous system. The agreement is very good, indicating that simple models can capture relevant features of CO_2/brine behavior.

Optimum perforation interval

When CO_2 injection commences, there is a difference in density between wellbore contents (CO_2) and reservoir fluid (brine), as sketched in the upper panel of Figure 5. Consequently, there is higher pressure difference between wellbore and reservoir at upper perforations compared to lower perforations. The variation can be significant in a thick aquifer. Therefore upper perforations inject more CO_2 in aquifer compared to lower perforations. Thus the CO_2 saturation increases faster in the upper part of the perforated interval. This increases relative permeability of CO_2 near upper perforations, and the fluid density profile in the near-wellbore reservoir also changes. The increase in relative permeability reduces the pressure difference required for injection, making the well pressure profile and reservoir pressure profile to come closer, as shown in middle panel of Fig. 5. The density change in reservoir fluid reinforces this effect. These competing effects may lead to some of bottom perforations becoming inactive after some time, bottom panel of Fig. 5. This phenomenon can be reinforced or mitigated by the nature of the relative permeability curves (Park, 2007). The effect is amplified as the injection rate per unit length of perforated interval decreases, so small injection rates in thick aquifers are the most likely to show a skewed vertical distribution of injected CO_2.

The vertical distribution affects both the lateral extent of the plume and the time to reach the top seal. Considering these effects, an optimum perforation interval for reducing these risk factors can be selected for a given injection rate. Figure 5 shows the simulation output the same effect and schematics showing the reason. The algorithm proceeds as follows:

Pressure in well at depth z = $P_{wt} + \rho_{CO_2} gz$ ……A1

Pressure in reservoir at depth z = $P_{rt} + \rho_w gz$ ……A2

where P_{wt} is the pressure at well top and P_{rt} is the pressure at reservoir(aquifer) top. Eqs. A1 and A2 lead to

$$\Delta P = \left(P_{wt} - P_{rt}\right) - \Delta\rho gz \qquad \text{……..A3}$$

where $\Delta\rho = \rho_w - \rho_{CO_2}$

The two curves intersect where

ΔP =0

i.e. at a depth z given by

$$z = \frac{P_{wt} - P_{rt}}{\Delta\rho g} \qquad \text{……A4}$$

If H>z, all the perforations are active.
Let us consider a small thickness Δz at depth z from reservoir top. Rate of injection across Δz is

$$\Delta q_{CO_2} = \Delta q_w = -\frac{kk_{rw}\left(2\pi\Delta P\right)\Delta z}{\mu \ln\left(\frac{r}{r_w}\right)} = -\frac{kk_{rw}}{\mu \ln\left(\frac{r}{r_w}\right)} 2\pi\left\{\left(P_{wt} - P_{rt}\right) - \Delta\rho g z\right\}\Delta z \quad \text{.....A5}$$

For $\Delta z \longrightarrow 0$

$$dq_{CO_2} = -\frac{kk_{rw}}{\mu \ln\left(\frac{r}{r_w}\right)} 2\pi\left\{\left(P_{wt} - P_{rt}\right) - \Delta\rho g z\right\} dz$$

$$Q_T = \int_0^Z dq_{CO_2} = \frac{kk_{rw}}{\mu \ln\left(\frac{r}{r_w}\right)} 2\pi\left\{\left(P_{wt} - P_{rt}\right) Z - \Delta\rho g \frac{Z^2}{2}\right\} \quad \text{if Z<H} \qquad \text{.....A6}$$

$$= \frac{kk_{rw}}{\mu \ln\left(\frac{r}{r_w}\right)} 2\pi\left\{\left(P_{wt} - P_{rt}\right) H - \Delta\rho g \frac{H^2}{2}\right\} \quad \text{if Z>H}$$

To determine P_{wt}

1. Start with $P_{wt} > P_{rt}$ and calculate Z from equation A4
2. Calculate Q_T from equation A6
3. If Q_T < Rate of injection, increase P_{wt} to next higher step and repeat step 1 and 2. If Q_T > Rate of injection, decrease P_{wt} to a lower value and repeat steps 1 and 2.

After small time step Δt, over which rate through Δz is constant, we have:

Volume injected = $\Delta q_{CO_2}\ \Delta t$

Saturation of CO_2 in Δz element = $\dfrac{\Delta q_{CO_2}\Delta t}{\pi\left(r^2 - r_w^2\right)\Delta z\phi}$

CO_2 relative permeability $k_{rg} = f\left(S_{CO_2}\right)$

Also after Δt time step the pressure profile in well will change due to change in density:

$\rho_z = S_{CO_2}\rho_{CO_2} + (1 - S_{CO_2})\rho_w$ where S_{CO_2} is a function of z.

Thus we update:

Pressure in reservoir = $P_{rt} + \rho_z g z$

Pressure in well = $P_{wt_n} + \rho_{CO_2} g z$

Now Z, dq and Q can be calculated in similar way as earlier but with new relative permeability and density.

Since from start more CO_2 is being injected in upper perforations, CO_2 saturation and CO_2 relative permeability is higher in upper perforations, decreasing the required ΔP and thus reducing Z. This may result in part of perforation becoming inactive. On the repeated calculation during injection period, the fraction of contributing perforations over time is determined. Thus perforation can be optimized by placing right amount of perforation at bottom of aquifer. This will increase the distance of top perforation from top seal and thus reduces the risk of hitting the top.

Risk reduction with horizontal well compared to vertical well

The performance of horizontal well vs. vertical well depends upon parameters such as horizontal length and vertical permeability. For a given injection rate, distribution of total flow along greater horizontal length reduces the velocity of plume. It also allows more CO_2 and brine/rock contact along the well length compared to vertical well. But on the other hand, due to lower velocity (higher gravity number), gravity forces can play a more dominant role, to the extent of making the flow almost vertical. This leads to less contact with brine and rock in the horizontal direction. In other words the horizontal well allows more trapping along the well but cannot take much advantage of permeability anisotropy to enhance trapping in horizontal direction. Thus the effectiveness of a horizontal well for reducing risk depends upon horizontal length and vertical permeability.

Figure 6 shows shape of CO_2 plume in an aquifer with a vertical well and then with a horizontal well. In this case the vertical well is 100 ft long whereas horizontal well is 1000 ft long. The horizontal spread is larger for the vertical well. For same rate of injection, the plume hits the top in 17 years in vertical well case and in 19 years in horizontal well case. Figure 7 shows the effect of horizontal well length on time to hit top seal. For lengths between 200 ft and 1000 ft there is no substantial increase in time to hit the top. The reason is explained above: there is competition between the reduced plume velocity and increased gravity number of the displacement. For a length of 2500 ft, the plume is in contact with more brine and rock and the velocity is reduced so much that it takes much longer to hit the top seal. On the same plot is shown the vertical well case. Plume in case of vertical well with 100 ft perforation takes longer time to reach top compared to 200ft and 300ft horizontal well.

Conclusions

- A certification framework is essential for establishing simple guidelines to follow before finalizing a geological site as candidate CO2 storage site.
- Operating parameters need to be decided based on their effect on acceptable risk thresholds.
- Simplified models of the effect of basic aquifer properties on plume migration can be developed.which capture behavior adequately for purposes of a certification framework

- Inhomogeneous systems can be replaced by equivalent homogeneous system.

Acknowledgement
This research was supported by the CO2 Capture Project Phase 2 (CCP2).

References

1. H. Haldorsen, L.W. Lake: “A new approach to shale management in field-scale models”, SPE 10976, 1984.
2. M.H. Holtz: “Residual gas saturation to aquifer influx: A calculation method for 3D-computer reservoir model construction”, SPE 75502, 2002.
3. Ide, M., K Jessen and F.M. Orr, “Time Scales for Migration and Trapping of CO2 in Saline Aquifers,” *Proc. 8th Int. Conf. Greenhouse Gas Control Technologies*, Trondheim, Norway, June 2006.
4. A. Kumar, R. Ozah, M. Noh, G.A. Pope, S. Bryant, K. Sepehrnoori and L.W. Lake: “Reservoir simulation of CO2 storage in deep saline aquifers”, SPEJ (Sept. 2005), pages 336-348.
5. Park, S.-Y., MS Thesis, The University of Texas at Austin, 2007.
6. K. Pruess, J. Garcia: “Multiphase flow dynamics during CO2 disposal into saline aquifers”, Environmental Geology(2002) 42, pages 282-295.
7. D. Silin, T.W. Patzek, S.M. Benson: “Exact solutions in a model of vertical gas migration”, SPE 103145, 2006.
8. K.J. Weber: “Influence of common sedimentary structures on fluid flow in reservoir models”, J. Pet. Tech, March 1982, Page 665-72.

Table1: Generic Reservoir Parameters

FORMATION ROCK/FLUID PROPERTIES		Units	Range of values		
			High	Medium	Low
Anisotropy	k_v/k_h	--	1	0.03	0.001
Residual nonwetting phase saturation	$S_{g,r}$	--	0.8	0.5	0.2
Average saturation of CO2 between injection well and injection front	S_{mean}	--	1	0.6	0.2
Relative permeability of CO2 at displacement front	$k_{CO2,disp}$	--	1	0.5	0.1
Lateral correlation length of permeability	λ	m	∞ (layered)	100	0 (uncorrelated)
Dip angle (from horizontal)	α	°	20	5	0
Thickness	h	m	300	50	10
Average permeability (horizontal)	$<k_h>$	mD	1000	100	10
Average porosity	ϕ	--	0.40	0.20	0.10
FORMATION CHARACTERISTICS					
Depth	Z	m	3000	1000	100
Lateral distance from injector to top of nearest anticline	L	m	∞ (no structure)	2000	200
Thickness of caprock	h_{cap}	m	1000	100	10
OPERATIONAL PARAMETERS					
Number of vertical injection wells	N_{vert}	--	10	1	0
Number of horizontal injection wells	N_{horiz}	--	10	1	0
Mass of CO2 to be injected	M	ton	10^8	10^7	10^6
Injection period	t_{inj}	y	50	10	5
Fraction of formation thickness in which vertical well is completed	f_{perf}	--	1	0.5	0.25

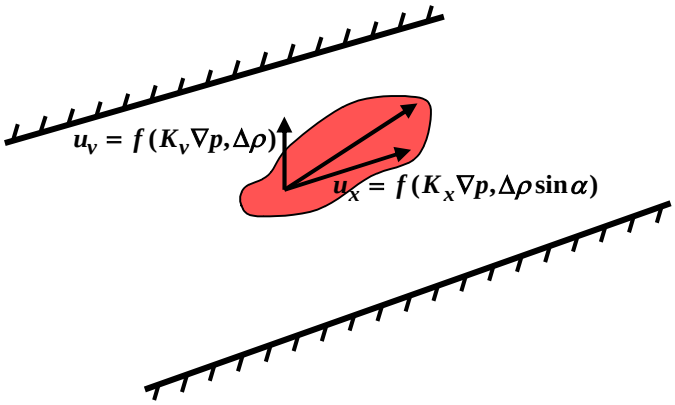

Figure 1: Schematic showing plume behavior in dipping reservoir

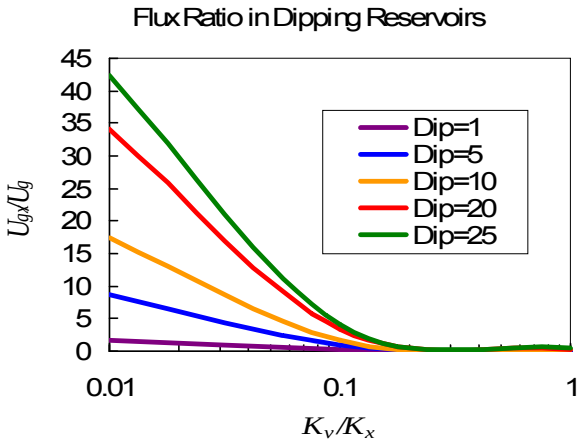

Figure 2: Flux ratio as a function of permeability ratio and dip angle

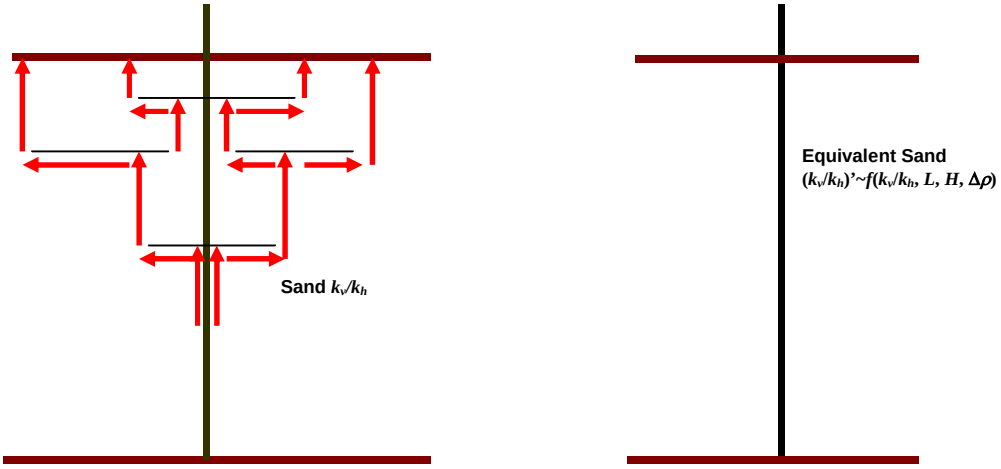

Figure 3: Plume direction in reservoir with imbedded shale barriers and its equivalent homogeneous model

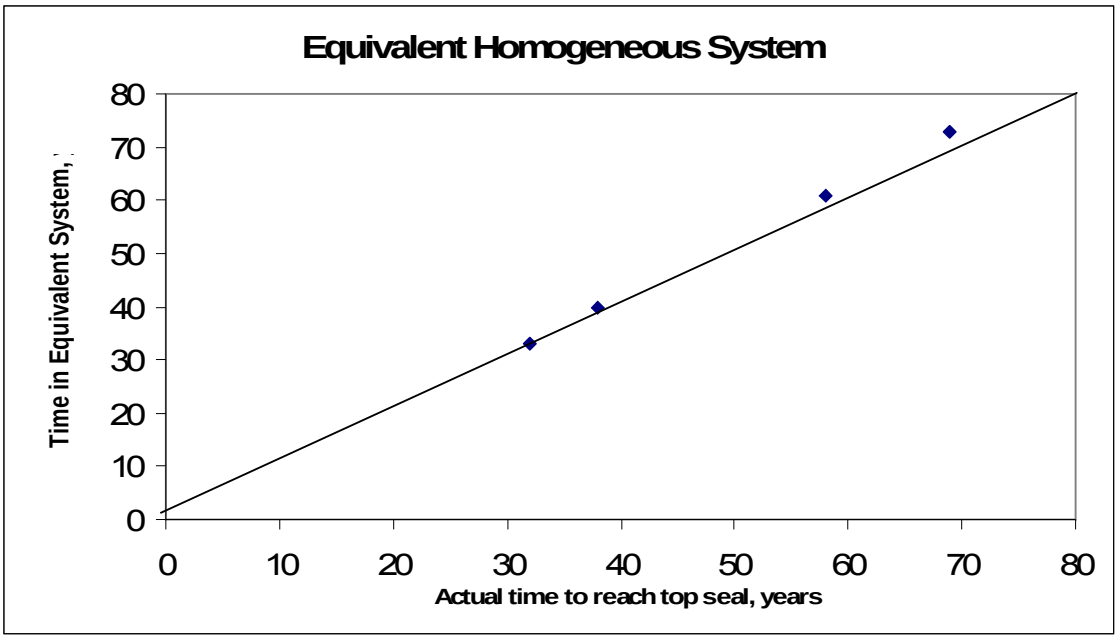

Figure 4: Time taken by plume to reach the top seal in shale imbedded aquifer and respective equivalent homogeneous system The equivalent system allows quick, inexpensive estimation of this response variable.

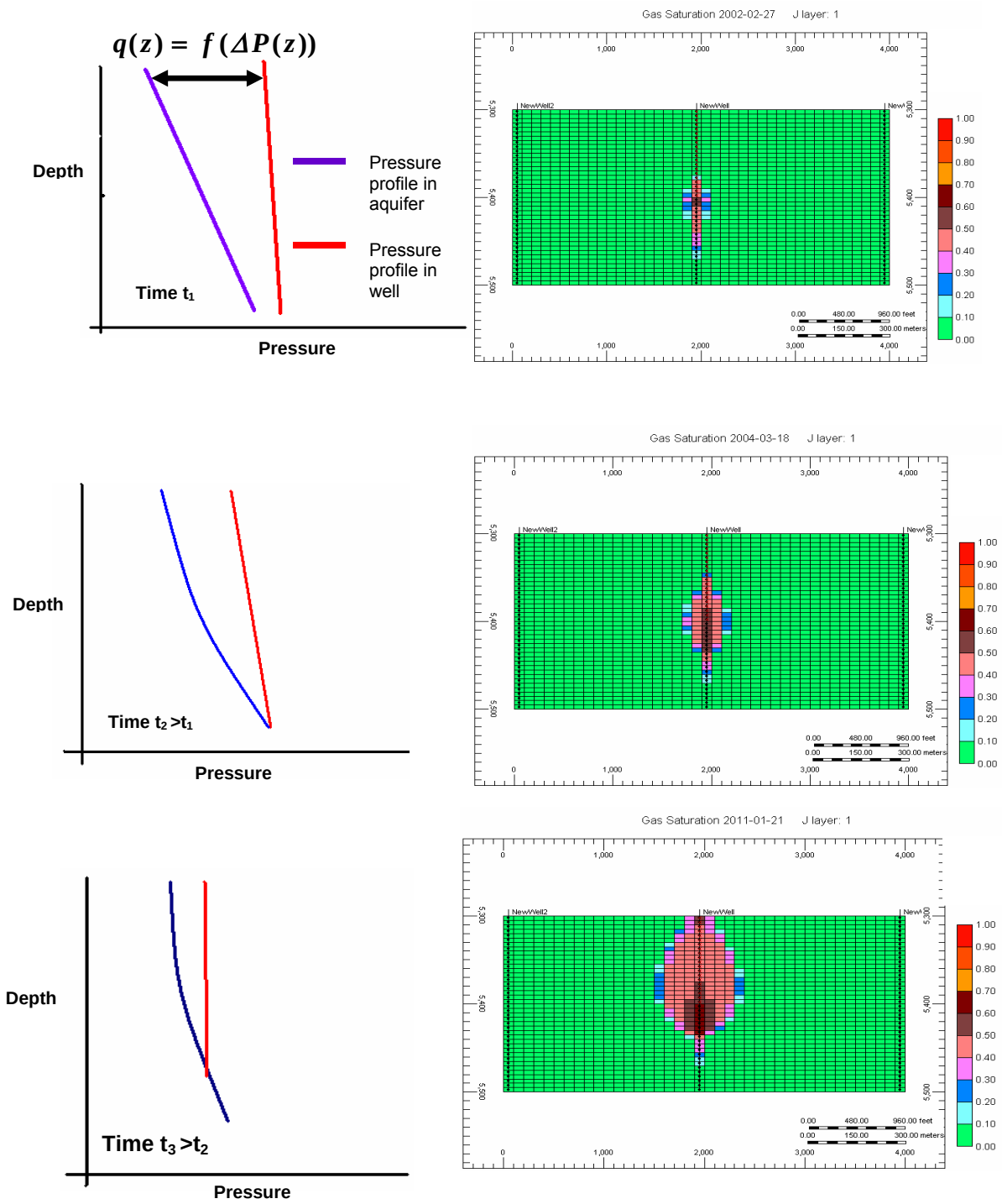

Figure 5: CO_2 distribution along the well length at three different times The different hydrostatic gradients in wellbore and in reservoir cause preferential flow of CO_2 into the upper perforations.

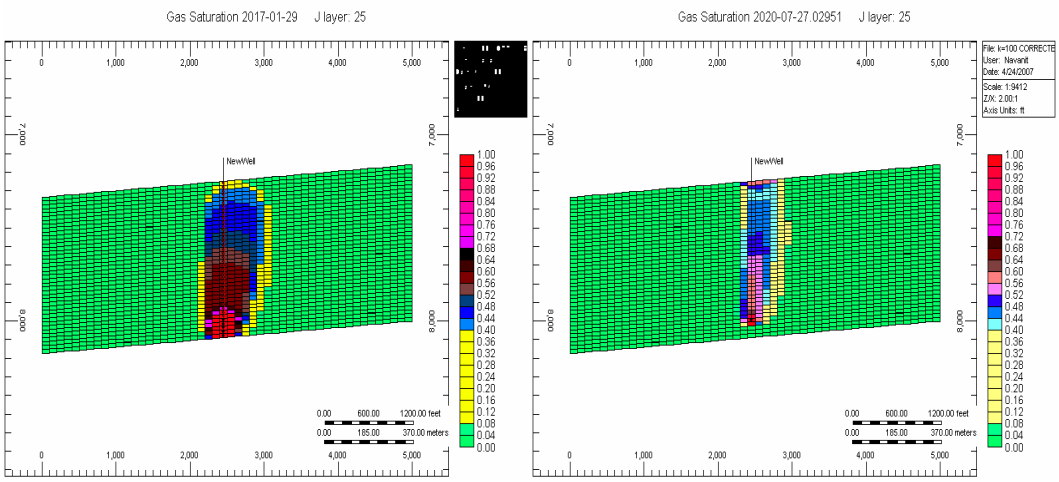

Figure 6: CO_2 plume shape in aquifer with (left) Vertical well (right) Horizontal well. Vertical well shows more horizontal spread compared to horizontal well. Horizontal well in figure is perpendicular to paper.

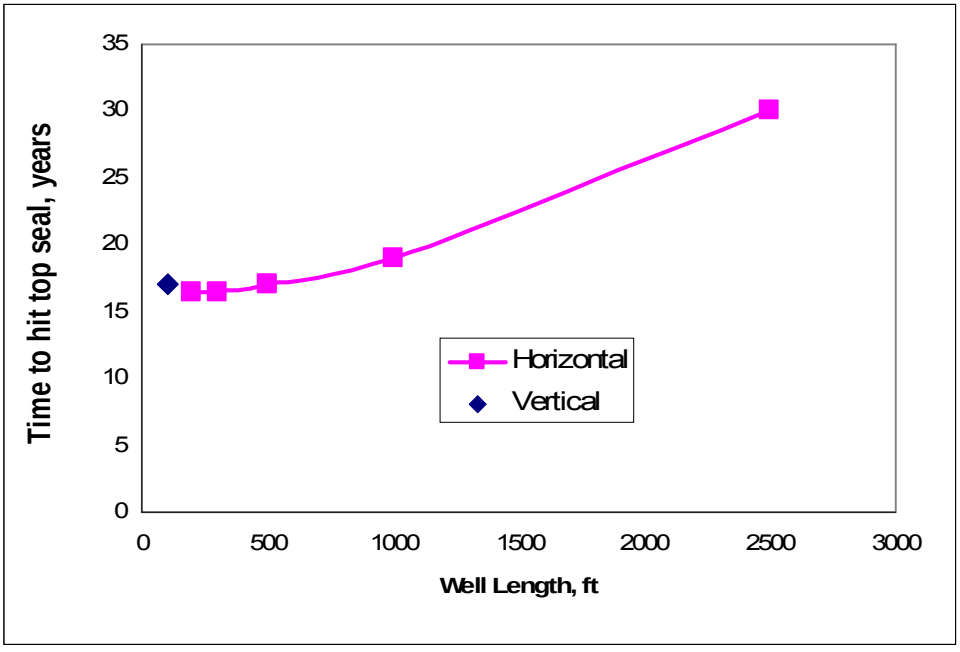

Figure 7: Effect of horizontal well length on time to hit top seal.